First attempt of the measurement of the beam polarization at an accelerator with the optical electron polarimeter POLO

B. Collin, J. Arianer, S.Essabaa
R. Frascaria, R. Gacougnolle, R. Kunne [1]

Institut de Physique Nucléaire/IN2P3
91406 ORSAY Cedex, France

K. Aulenbacher, V. Tioukine

Institut für Kernphysik
Johannes Gutenberg-Universität Mainz
55099 MAINZ, Germany

EXT-2004-056
11/06/2004

Abstract

The conventional methods for measuring the polarization of electron beams are either time consuming, invasive or accurate only to a few percent. We developped a method to measure electron beam polarization by observing the light emitted by argon atoms following their excitation by the impact of polarized electrons. The degree of circular polarization of the emitted fluorescence is directly related to the electron polarization. We tested the polarimeter on a test GaAs source available at the MAMI electron accelerator in Mainz, Germany. The polarimeter determines the polarization of a 50 keV electron beam decelerated to a few eV and interacting with an effusive argon gas jet. The resulting decay of the excited states produces the emission of a circularly polarized radiation line at 811.5 nm which is observed and analyzed.

Key words: polarimeter, fluorescence, electron beam, polarization
PACS: 07.60.Fs, 29.27.Fh, 33.50.Dq, 34.80.Nz

[1] Corresponding author, email: kunne@ipno.in2p3.fr

1 Introduction

The idea of measuring the polarization of low energy electron beams by observing the fluorescence emitted by mercury atoms following their excitation by polarized electron impact was suggested by Farago and Wykes in 1969[1]. Such a measurement was then first performed on zinc atoms by Eminyan and Lampel in 1980[2]. So far, improvements were achieved by considering the use of noble gases whose properties make it easier to handle the experimental apparatus and lead to more accurate results (better than 1%)[3–5]. However this optical method has not found wide applications since the figure of merit

$$FOM = \frac{S^2 N}{N_0}$$

is orders of magnitude lower than for conventionnal Mott polarimeters (S is the analyzing power, N/N_0 is the rate of detected events normalized to rate of incident primary electrons). On the other hand, for measurements at particle accelerators where the primary intensity of the electron beam is very high, an optical polarimeter would allow fast and accurate measurements at the full beam current of the experiment. It should be noted that such a device would offer a considerable improvement in comparison with current installations (Möller and Compton backscattering polarimeters) at particle accelerators like MAMI or JLAB, because these either cannot stand the full current on target due to target heating effects (Möller polarimeters[8]) or they need long measurement times (Compton backscattering[9]).

In this article we describe the operation of an optical polarimeter (POLarimètre Optique, POLO) together with an injection system for the MAMI accelerator. In its present design it is intended as an offline device, which would measure the polarization of the beam deflected from the 100 keV injection system of MAMI. First we review the theoretical aspects and describe the experimental set-up. Next, we state the results obtained and the perspectives of the experiment.

2 Theoretical aspects

2.1 General layout

Optical polarimetry is based on the inelastic exchange collision of polarized electrons on atoms :

$$\vec{e} + A \rightarrow \vec{A^\star} + e'$$

such that spin angular momentum is transferred to the excited atom. This excited atom eventually decays into a metastable state yielding the emission of circularly polarized light :

$$\vec{A^\star} \rightarrow A_m + (h\nu)_\sigma$$

The detection and analysis of the polarized fluorescence provide knowledge of the electron beam polarization. Although most of the noble gases might be used as target, we chose argon. Argon has a large cross-section and a high energy-gap between the threshold of the reaction (13.08 eV) and the first cascading state (13.90 eV). Is is also easy to pump and cheap. In the case of argon, the excited state is $(3p^5 4p)^3D_3$ which decays to $(3p^6 4s)^3P_2$ by emission of a 811.5 nm fluorescence line. Figure 1 shows the excited argon levels, including the excited ^3D_J states and radiative transitions to the ^3P_J. The first cascading state $(3p^5 3d)^3P_2$ is also shown.

The excitation process follows three steps :

(1) argon atoms are excited by polarized electrons from the beam, leading to spin transfer between the incident electrons and the argon atoms. The collision time is typically 10^{-15} s.
(2) relaxation of the fine structure of states $(3p^5 4p)^3D_J$ occurs in 10^{-12} s.
(3) the excited states decay to $(3p^5 4s)^3P_J$ in around 10^{-8} s, yielding in particular to the emission of the 811.5 nm radiation line[10].

The detection and subsequent analysis of the emitted light is subject to three conditions:

(1) the argon $^3D_3$ state must be directly excited (i.e. cascading from higher states must be avoided) to avoid any admixture of unknown polarization.
(2) any magnetic interaction of the incident electron which could cause its spin to flip must be negligible in the excitation process.
(3) spin-orbit coupling within the excited atom must be large enough to allow the fine structure splitting of the ^3P_J levels to have them easily spectroscopically resolved.

This favors the use of noble gases[11] and implies that the beam energy should lie between the excited state threshold (13.076 eV) and the energy of the first cascading state $(3p^5 3d)^3P_2$ (13.903 eV).

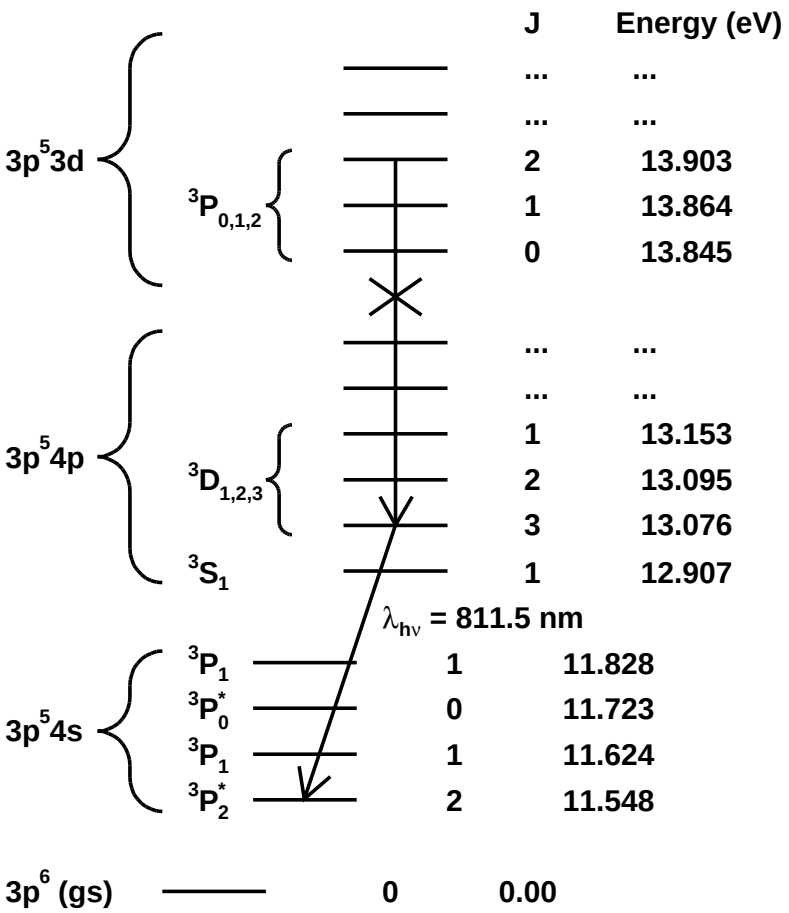

Fig. 1. Argon I spectrosopic levels.

2.2 Polarization and Stokes parameters

Fluorescence light is analyzed through its Stokes parameters which are related to the initial beam polarization[10,12]. For an incident transversally polarized beam on the z-axis, the fluorescence light is observed along the y-axis in the direction of the electron spin. The intensity of the circularly polarized light emitted per unit of solid angle is proportional to $1 + \cos^2\theta$, where θ refers to the angle between that direction of detection and the y-axis[1]. The intensity is therefore maximum in the spin direction. The linear and circular polarization are parameterized by the so-called Stokes parameters U, V and Q defined as follows (figure 2):

$$Q = \frac{I(0^o) - I(90^o)}{I(0^o) + I(90^o)} \quad V = \frac{I(\sigma^+) - I(\sigma^-)}{I(\sigma^+) + I(\sigma^-)} \quad U = \frac{I(45^o) - I(135^o)}{I(45^o) + I(135^o)}$$

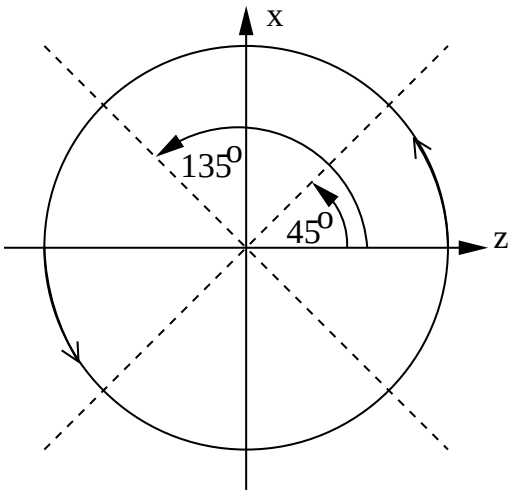

Fig. 2. Angles used in the definition of Stokes parameters.

where I(α) is the intensity of the polarized light along the direction having a polar angle α in the xz-plane and where $\sigma^{\pm}$ refers to right and left handed circularly polarized light. It was shown that for noble gases the beam polarization P is related to the reduced Stokes parameters by [11]:

$$V/I = A(1 + BQ/I)P \tag{1}$$

I being the incident intensity. This requires the condition U=0, which is obtained if the excited state is a well LS-coupled state (Russell-Saunders state) and if in addition the spin-orbit interaction between the target and continuum electrons is negligible during the collision process[13]. For the $^3D_3$ level of argon, the relation becomes:

$$V/I = 0.6667(1 + 0.2222Q/I)P \tag{2}$$

It should be noted that this relation is only valid in an energy range unaffected by cascades [11] and for a transverse spin [13].

3 Experimental set-up

The experimental apparatus (Fig. 3) consists of a six-way cross chamber in which the beam is decelerated to around 13 eV prior to interacting with an argon jet. The emitted fluorescence is then detected by an optical detection system and sent to the data acquisition system for analysis.

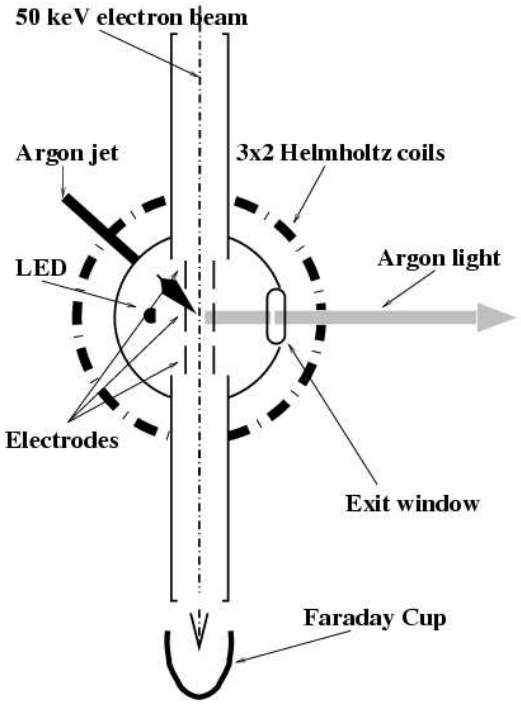

Fig. 3. Experimental apparatus (see text for details).

3.1 Polarized electron source

POLO was installed in the old polarized electron injection beamline of MAMI [14]. The beam from the polarized source which produces longitudinally polarized electrons is guided by a 10-meter long transport system towards a spin rotator [15]. The rotator is set to 90° spin rotation to provide for the necessary transverse spin orientation at POLO. In addition this mode of operation can be used to check the beam polarization with a conventional Mott polarimeter. Due to restrictions in the available space for the insulation of the deceleration stage (see section 3.2), the beam energy is reduced from 100 kV to 50 kV. With careful tuning an almost complete beam transmission ($\geq$98%) of the electron beam to the entrance of POLO is achieved. The average beam current at the experiment is chosen 20-25 μA which is a typical injection current for the A4-parity violation experiment at MAMI[16,17]. All experiments are performed with bulk GaAs photocathodes excited by a diode laser with circularly polarized light of wavelength λ=808 nm. Typical quantum efficiencies are 1%, resulting in a current capability of up to 100 μA. The beam polarization is determined by Mott measurement at 100 keV beam energy to be typically (28$\pm$1)%. The beam position in POLO is controlled by a viewscreen 30 cm in front of the polarimeter and can be manipulated by steering coils. The matching of the electron optical input parameters towards the optimal values for the deceleration optics (Fig. 4) is achieved with a symmetrically driven 'back-to-back'-solenoid. This technique of solenoid operation avoids any additional

spin rotation during focusing.

3.2 Beam deceleration

We extract the beam from the source with a kinetic energy of $T_{beam} = 50\,\mathrm{keV}$. This is necessary to achieve a reasonable magnetic rigidity during the 10 m long beam transport to the experiment. On the other hand this is reasonably close to the kinetic energies found in the injection systems of electron accelerators. The reason for choosing 50 instead of 100 keV are that the internal as well as the external spaces for electrical insulation were insufficient.

The kinetic energy has to be reduced in the interaction region to energies close to the threshold of the argon transition, therefore $T_{inter} = 0 - 100\,\mathrm{eV}$.

Due to the limited space in the vacuum chamber the beam deceleration is performed in a single 30 mm wide gap between two cylindrical brass tubes of 20 mm inner diameter (figure 4, where the beam enters from the left with T_{beam}). In the middle of the 115 mm long interaction tube the electron beam overlaps with the argon jet.

The interaction tube is held at a potential of $-T_{beam}/e + \Delta$, by connecting the negative input of an insulated (floating) power supply -the socalled scanner - with the the high voltage of the source. This eliminates drifts of the high-voltage power supply. The battery powered scanner provides the variable voltage $\Delta = 10 - 100\,\mathrm{V}$ which defines the interaction energy T_{inter}. The scanner is remote-controlled via fiber optics.

The fluorescence signal may escape by an aperture machined into the cylinder. It is covered by a metallic mesh in order to maintain a well defined potential at the position of the argon jet.

Because of the large ratio $T_{beam}/T_{inter} \approx 2500$ it has to be expected that the electrostatic lens which is formed by the deceleration gap has a short focal length. The computersimulation of the beam which was performed with the SLAC Electron Transport Program[18] (figure 4) shows that the focal length is about one centimeter.

Even with the small input emittance (at $T_{beam} = 50\,\mathrm{keV}$) of $\epsilon = 1\pi$ mm mrad and optimized matching by the external solenoid it is not possible to achieve complete transmission through the interaction region. This restricts the use of the polarimeter in its present set-up to offline operation. In addition the overlap with the argon jet is not optimized.

In the future the problem of short focal length may be controlled by introduc-

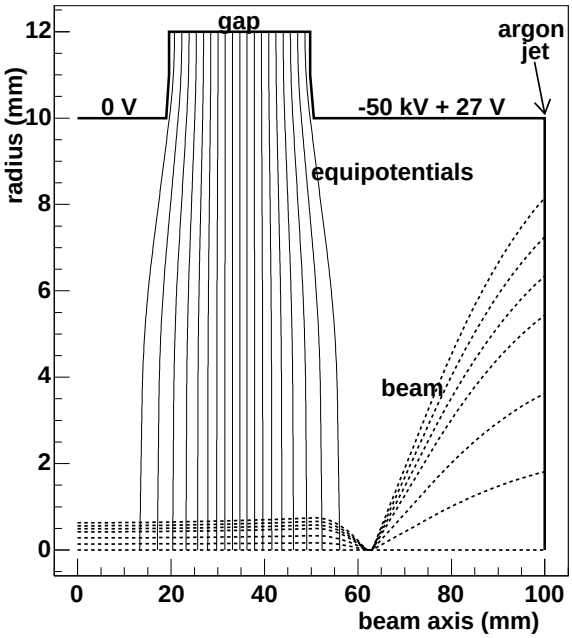

Fig. 4. Simulation of electron transport: R=0.75 mm, d=-2.5 mrad, g=3 cm (only half of the decelerating electrode is shown). The vertical solid lines represent equipotential lines in the gap between the electrodes (left: ground electrode 0 V, right: decelerating electrode -50 kV+27 V) and the dashed lines show electron trajectories. Argon is injected in the middle of the decelerating electrode.

ing a multistage deceleration which increases the focal length in each stage because of the lower ratio of kinetic energies.

The fraction of the beam which is transmitted through the interaction region, is again reaccelerated in an identical 30 mm gap in order to achieve a measurement of beam transmission at the Faraday cup.

In the interaction region of POLO, the earth magnetic field components were measured to be :

$$B_x = 22\mu T \qquad B_y = 6\mu T \qquad B_z = 34\mu T \tag{3}$$

resulting in a 41 μT total field. This field is compensated with three sets of Helmholtz coils to a level below 1.8 μT. This eliminates the possibilities of relevant spin precession during the passage of the electron beam through POLO and prevents from depolarization by Hanle effect [19]. On the other hand the effects of spin precession during the transport over a distance of about 2 m from the spin rotator (and the Mott polarimeter) to POLO cannot be completely eliminated and may be partly responsible for the observed deviation

of the asymmetry from the value that would correspond to the polarization measured by the Mott polarimeter. This is discussed in more details in section 5.

3.3 Argon jet

The argon atoms are injected in the interaction region as an effusive jet produced by a 30 mm long nozzle with 0.2 mm diameter. It was measured to have a conical shape with 29° half angle at the top.

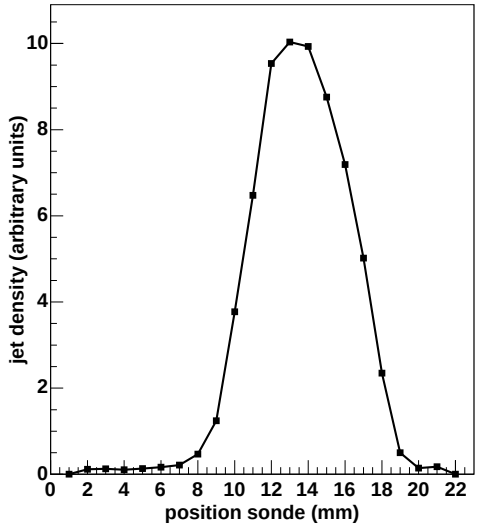

Fig. 5. The shape of the argon jet as measured by a capillary sonde.

The pumping system consists of a cryogenic pump of 640 ls^{-1} mounted on the chamber. A turbopump coupled to a primary pump is installed higher on the beam line to improve the pumping power and protect the beam line vacuum. A vacuum of 10^{-7} mbar is achieved and a pressure of argon up to $4x10^{-5}$ mbar is maintained during operation.

3.4 Optical detection

The analysis of the emitted fluorescence light is done through a measurement of its Stokes parameters. The circularly polarized fluorescence light is analyzed by an optical system (Fig. 6) consisting of a quarter-wave plate and a polarizer. A interferential filter is used to select the 811.5 nm radiation line. The filter has a band width of 1 nm centered at the transition wavelength of 811.5 nm and can therefore suppress the contribution of an adjacent transition at 810.4 nm. However during analysis of our data we found that the

converging beam profile passing through the filter causes a shift of the transmission maximum towards the background transition. For this reason we have a non-negligible background contribution which is discussed in section 5. A set of lenses is used to focus the fluorescence light which is then collected by an Oriel Instruments 77348 photomultiplier (3 nA dark current, 15 mA/W photocathode sensitivity).

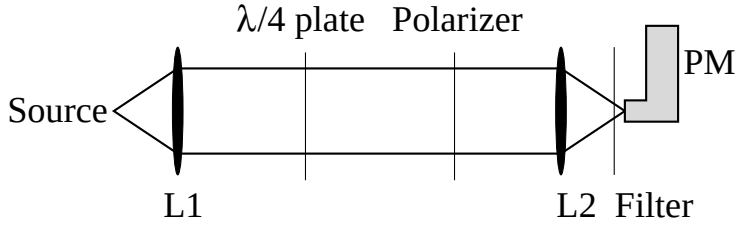

Fig. 6. Optical bench.

The polarizer is set to a fixed position α and the quarter-wave plate is rotated by fixed steps of 15°. In these conditions, the detected intensity for each position θ of the quarter-wave plate is

$$I_d(\theta) = \frac{I}{2} + \frac{Q}{4}(\cos(4\theta - 2\alpha) + \cos(2\alpha)) - \frac{U}{4}(\sin(-4\theta + 2\alpha) + \sin(2\alpha)) + \frac{V}{2}(\sin(-2\theta + 2\alpha)) \quad (4)$$

This detected intensity corresponds to the counting $\mathrm{N}^+(\theta)$ associated with the right helicity of the beam polarization. If the spin is flipped at the source, the counting $\mathrm{N}^-(\theta)$ for the left helicity is such that $\mathrm{N}^-(\theta)$=$\mathrm{N}^+(\theta$+90°). The asymmetry

$$A_\theta = \frac{N^+(\theta) - N^-(\theta)}{N^+(\theta) + N^-(\theta)} \quad (5)$$

is then related to the reduced Stokes parameters :

$$N^+(\theta) - N^-(\theta) = \sin(-2\theta + 2\alpha)\frac{V}{I} \quad (6)$$

$$N^+(\theta) + N^-(\theta) = I_\theta = \frac{1}{2}(\cos(4\theta - 2\alpha) + \cos(2\alpha))\frac{Q}{I} - \frac{1}{2}(\sin(-4\theta + 2\alpha) + \sin(2\alpha))\frac{U}{I} \quad (7)$$

3.5 Data acquisition

The data acquisition system is remotely controlled, as it is not possible to access the polarimeter while the GaAs source is running. It consists of a fast amplifier, a discriminator and a CAMAC scaler and follows four steps:

(1) the polarized 50 keV electron beam is driven from the GaAs source to the entrance of POLO (the beam polarization is measured at the source by a Mott polarimeter). The deceleration of the beam to the energy threshold is operated by adding a variable voltage ΔV to the -50 kV of the decelerating electrode by means of the scanner. The same 50 kV are applied to the extraction gun and the decelerating electrode to avoid any voltage offset.
(2) the polarizer is set to a fixed position α and the quarter-wave plate is remotely rotated from a PC by fixed steps of 15° every 200 seconds to allow sufficient statistics.
(3) for each position θ of the quarter-wave plate the output signal of the photomultiplier is sent to the amplifier where it gets amplified to above 100 mV. A discriminator is used to set the threshold and its output is directed into a CAMAC scaler. Both countings $N^{\pm}(\theta)$ are done simultaneously by flipping the spin every second by a Pockels cell at the source (this minimizes the impact of slow drifts of the signal and avoids any correlation of the intensity with external noise of any frequency). The beam current is measured on the Faraday cup and fed into a current to frequency converter, whose output is also connected to the scaler. This allows to normalize the count rates to the beam current.
(4) the asymmetry is calculated from the count rates for each position of the quarter-wave plate.

4 Inelastic collision signature

One of the most difficult points of the experiment is the deceleration of the electron beam. Due to lack of space the 50keV electrons are decelerated over a distance of only 13mm. The severe focusing disperses the beam in the interaction region and leads to a low signal of fluorescence. The transmission as measured by the Faraday cup after the interaction region is of the order of 5%.

The first step in these conditions is to observe the clear signature of the interaction between the electrons and the atoms. This was realized by observing the full argon spectrum with the use of a monochromator (Jobin-Yvon HR320) at a deceleration voltage of 25 V for a measured beam intensity of 1 μA at the

Faraday cup. The spectrum (Fig. 7) was obtained with relatively large slits on the monochromator to favor light collection. This configuration of the detection system does not allow to spectroscopically resolve the 7504-7515 and 8104-8115 lines. The signal/background ratio is roughly 1 for the more intense peaks. It was proved that the origin of the background is purely due to the photomultiplier anode dark current (around 3 nA), showing that the measured signal is much lower than expected. The reduction can be partly explained by the low monochromator transmission (≈50%) and Fresnel losses.

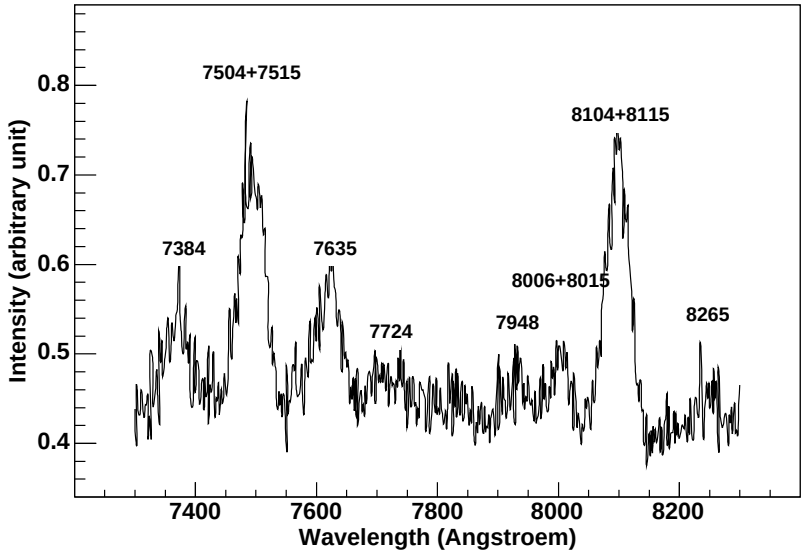

Fig. 7. Argon spectrum. Theoretical wavelengths are quoted on top of each peak.

The second step consists in measuring the excitation function of the $^3D_3 \rightarrow ^3P_2$ fluorescence light (Fig. 8). The excitation function is obtained by measuring the intensity of the 811.5 nm peak at different beam energies, i.e. at different deceleration voltages. The error bars account for the accuracy in extracting the peak amplitude out of the background. This result is in agreement with a previous measurement by Gay et al. [4].

5 Signal over background ratio and measurement speed

The signal was optimized by varying the focusing strength of the final solenoid and the steerer currents in front of POLO until a maximum of the signal occured. A transmission of 40% was obtained.

At the peak of the excitation function (fig. 8) we observed a signal rate of $R_0 = 35$ kHz for a primary electron current of 25 μA. Under this conditions

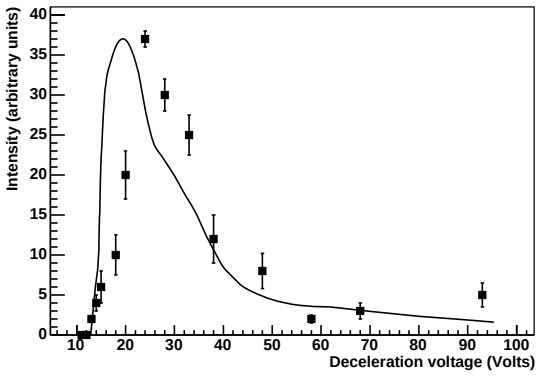

Fig. 8. Excitation function of the argon 811.5 nm radiation line $^3D_3 \rightarrow ^3P_2$. The experimental points are compared to a fit of data measured by Gay et al. (see text)

the time needed to achieve a statistical accuracy below one percent in less than one minute.

Our result may be compared to a value given by Trantham et al. [5], who achieved 1 kHz/μA at the peak energy for a Neon transition with a similar detection system and with good overlap between the gas jet and electron beam. Taking into account the ratio of cross sections, gas pressures and typical photomultiplier efficiencies we find that our efficiency is about 30% of theirs. This is due to the large diameter of the beam in the interaction region (see fig. 4) which leads to a reduction of luminosity.

A constant background of 600 Hz resulted from the photomultiplier dark current. The operation of the high energy beam leads to parasitic emission of light which generates a background which is proportional to the electron current. This was measured (without argon in the chamber) as 0.4 kHz at 25 μA. The sum of these two background terms was subtracted as unpolarized contribution in the measurements discussed below.

Another background source which is more difficult to estimate is the generation of light by secondary electrons formed by the transmission loss on the POLO electrode. Since these electrons may loose their polarization in the backscattering process they dilute the polarization signal. An estimation of the total number of these processes may be given by the available data on the secondary electron multiplication coefficient δ which should be around $\delta = 0.1$ in our energy range. It may be increased by the large angle of incidence of the loss electrons and by the not very well defined state of the brass surface by less than a factor of five, so we estimate $\delta^* < 0.5$ [21].

It is known [6] that at energies of $T_{inter} < 30$ V a considerable fraction q of the order of 30% of the secondary electron emission may consist of elastically scattered electrons, whereas the low energy part of secondary emission is not

harmful since it falls below the threshold of the argon transition. Therefore we estimate the rate of events which are caused by secondary electrons to:

$$R_{sec} \leq q\delta^* L R_0 \rightarrow R_{sec} < 0.1 R_0 \tag{8}$$

where $L < 0.6$ is the transmission loss.

A last background contribution , the 'optical background', is due to the shift in the interference filter frequency mentioned in section 3.4. which can be calculated to be of the order of 0.3 nm. Taking into account the parameters of the filter we find that the background from the 810.4 nm line might have a relative transmission of $T_B \approx 0.2$ at most, with respect to the signal. The intensity of the background with respect to the signal is given by the ratio of the electronic cross sections of the two transitions which is of the order of 1 [20].

No attempt has been made to correct the experimental asymmetries for the background terms of secondary electrons and the optical background.

Summing up all background contributions,we find that our signal to background ratio is $S/B \approx 2$. All background sources may be reduced by at least an order of magnitude by taking appropriate measures like photomultiplier cooling, adjusting of the interference filter, and designing an electron optics with better transmission.

6 Spin transfer and Stokes parameters measurement

Strictly speaking, the relation between the beam polarization and the Stokes parameters given in section 2.2 is only valid below the energy levels of the cascading states. However, at 29.5 ± 1.5 eV the cross-section is about 25 times larger than at 13.9 eV and a substantial fraction of the polarization is still transfered from the electrons to the photons, leading to a much better figure of merit. At this value the transmision is improved as well : we achieved a transmission of 40%.

One of the measurement is shown in figure 9. A fit and χ^2 minimization on data (corrected from background) using the four parameter function of section 3.4 for asymmetry A_θ leads to the following reduced Stokes parameters:

$$Q/I = (7.7 \pm 5.2)\% \qquad U/I = (0.6 \pm 3.8)\% \qquad V/I = (11.2 \pm 0.2)\% \tag{9}$$

It is obvious that in spite of the high statistical accuracy of the data points a good extraction of the parameters U and more importantly Q is not possible.

The present error on Q implies a relative error of 1.1% in extracting the polarization P from the generic equation in section 2.2 (cf. equation 2) which is more than the expected better-than-1% value. More precise measurements of U and Q are possible by determining I_θ (cf. equation 7) and extracting the parameters by a Fast Fourier Transform analysis. Due to the very complicated and extended electron optical system in front of POLO we have not yet been able to achieve a sufficiently accurate result for I_θ, whereas A_θ can be measured easily thanks to high spin flip frequency.

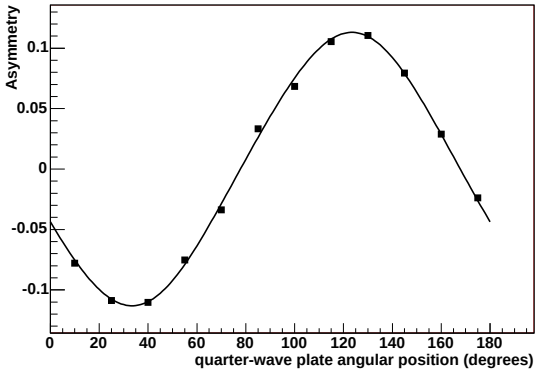

Fig. 9. Corrected asymmetry fitted by the parametrisation of equation 5.

From the measured Stokes parameters it is not straightforward to calculate the beam polarization since equation 2 is only valid at threshold and the measurement was performed at 29.5 eV where cascading from higher states can modify the polarization of the $(3p^5 4p)^3D_3$ excited state. However, the beam polarization was measured at the exit of the source with a standard Mott polarimeter and found to be 28%. The values of U/I, Q/I and V/I at 29.5 eV for a beam polarization of 28% can be inferred from Furst et al. [11]:

$$Q/I \approx 15\% \qquad U/I = 0\% \qquad V/I \approx 16\% \tag{10}$$

Our measured value V/I differs by about 30% from the value measured by Furst et al.. We believe that the major part of this deviation is explained by the background contributions discussed in section 5. A smaller, but non-negligible correction of a few percent is due to a possibly not completely transverse spin orientation.

The errors resulting from the uncertainties in the corrections are too large to give a reasonable self-calibration of the device. Therefore in its present form the polarimeter has to be calibrated with another polarimeter, i.e. the Mainz Mott polarimeter. The main issues are therefore a reduction of the backgrounds as outlined in section 5, which will then allow a more accurate measurement of the curve I_θ.

Besides still-to-tackle technical difficulties one can anyway draw some promising conclusions about the optical measurement:

(1) it is very sensitive to the value of V/I and the fit analysis provides an accuracy on V/I of around 0.2%.
(2) the measurement time is 200 seconds for each position of the quarter-wave plate resulting in a forty minute measurement to reconstruct the whole asymmetry curve. This time could be lowered by improving the signal/background ratio and by using a Fast Fourier Transform (FFT) to analyse the fluorescence light.
(3) once the polarimeter is calibrated, measurements can be done by taking data at the highest asymmetry $A_\theta{}^{max}$. The maximum asymmetry we reached in our experiments is $A_\theta{}^{max}$=12.5%. At a rate of 35kHz it it possible to measure this value with a statistical accuracy of $\delta A_\theta/A_\theta \leq 1\%$ in less than 20s, which would again be reduced by one order of magnitude if a strained layer cathode delivering 80% of polarization (e.g. three times larger asymmetry) was used. Defining ten minutes as an acceptable measurement time for a polarization measurement - which must not be too time consuming as the physics experiment must be stopped during offline measurements - this offline optical polarimeter would be useful in a current range I$\geq$40 nA which is far below the current used by most hadronic physics experiments (except for some with real photons). Therefore its dynamic range is well suited to the needs of hadronic physics.

7 Conclusions and perspectives

We have demonstrated the operation of the POLO optical polarimeter in the injection system for a high energy particle accelerator. An advantage of this gas-target system for an accelerator lies in the fact that it can be operated at the typical intensities relevant for hadronic physics experiments. Precise measurements could be performed in very short times. In its present state the polarimeter needs a calibration with an existing high accuracy polarimeter (e.g. Mott polarimeter).

Future work will have to focus on self-calibration of the polarimeter, a procedure that has been demonstrated to reach accuracies below 1%. The increase to 100 keV injection and the construction of a deflection system from the injection beamline in MAMI would not pose major problems but it requires considerable engineering effort.

References

[1] P. S. Farago and J. S. Wykes, *J. Phys.* **B2**, 747 (1969).

[2] M. Emynian and G. Lampel, *Phys. Rev. Lett.* **45**, 1177 (1980).

[3] T. Gay et al., *J. Phys.* **B16**, L553 (1983).

[4] T. Gay et al., *Phys. Rev.* **A53**, 1623 (1996).

[5] K. W. Trantham et al., *Rev. Sci. Instrum.* **67**, 4103 (1996).

[6] G. A. Harrower, *Phys Rev.* **104**, 52 (1956).

[7] G. A. Harrower, *Phys Rev.* **106**, 1 (1956).

[8] H. Hauger et al., *Nucl. Instr. and Meth.* **A462**, 382 (2001).

[9] T. Pussieux et al., *Proceedings of the 14th International Symposium on High Energy Spin Physics, Osaka, Japan*, 761 (2000).

[10] G. F. Hanne, *Phys. Rep.* **95**, 95 (1983).

[11] J. E. Furst et al., *Phys. Rev.* **A47**, 3775 (1993).

[12] J. E. Furst et al., *J. Phys.* **B25**, 1089 (1991).

[13] K. Bartschat and K. Blum, *Z. Phys.* **A304**, 85 (1982).

[14] K. Aulenbacher et al., *Nucl. Instr. and Meth.* **A391**, 498 (1997).

[15] K.-H. Steffens et al., *Nucl. Instr. and Meth.* **A325**, 378 (1993).

[16] F.E. Maas (A4-Collaboration), *Eur Phys J.* **A17**, *339-343 (2003)*

[17] B. Collin, *Ph.D Thesis, ParisXI-Orsay University* (2002).

[18] W. B. Herrmansfeldt, *Electron Transport Program SLAC Report 166* .

[19] G. Fishman and G. Lampel, *Phys. Rev.* **B16**, 820 (1977).

[20] J. K. Ballou et al., *Phys. Rev.* **A8**, 1797 (1973).

[21] R. Kollath, in *Handbuch der Physik*, edited by S. Flugge Springer-Verlag, Berlin, (1956), Vol. 21